ACI STRUCTURAL JOURNAL TECHNICAL PAPER

Title no. 99-S47

Retrofitting of Concrete Structures for Shear and Flexure with Fiber-Reinforced Polymers

by Shamim A. Sheikh, David DeRose, and Jamil Mardukhi

Damage sustained by foundation walls and large beams in a building was simulated in full-size to near-full-scale model specimens in the laboratory. The damaged specimens were repaired with carbon and glass fiber-reinforced polymer (CFRP and GFRP) sheets and wraps, and tested to failure. Companion control specimens were also tested to failure without rehabilitation to provide a basis for comparison and evaluate the effectiveness of the repair techniques. Test results showed that fiber-reinforced polymers (FRPs) were effective in strengthening for flexure as well as shear. Over-reinforcing in flexure resulted in shifting the failure to shear mode, which in some cases may be undesirable. Strengthening of a member in shear, on the other hand, resulted in increasing the ultimate displacement by more than tenfold, and toughness by a factor of more than 26. Available analytical procedures and building code provisions were found to simulate the behavior of specimens retrofitted with FRP reasonably well.

Keywords: fibers; flexure; polymer; shear.

INTRODUCTION

The upgrading of existing structures is an integral part of structural engineering practice and requires a dedicated solution to a problem at hand. Retrofitting may be required to strengthen the structures either damaged by environmental effects or that need to meet new code requirements. There are always design- and construction-related deficiencies that need to be corrected. Steel and cementitious materials are commonly employed for most of the retrofitting work, but they have not always proved effective, durable, or economical. Due to the heavy weight of the materials, these techniques are equipment- and labor-intensive. The duration of repair may also be quite long, often requiring the facility to close for a long period of time, which could be very costly. In the case of bridges and other transportation structures, the duration of repair time is a particularly critical factor in the decision-making process. In many situations, retrofitting with fiber-reinforced polymers (FRPs) provides a more economical and technically superior alternative to traditional techniques. FRPs are lighter, durable, and have higher strength-to-weight ratios than traditional materials such as steel. Working with FRP is, therefore, less labor- and equipment-intensive, which can shorten the time required for retrofitting and allow the construction to proceed without closing the facility.

In this study, the use of FRP in the repair of beams, slabs, and walls is investigated. The test program was inspired by a high-rise structure that consisted of a multistory apartment building built over a number of parking levels. Extensive cracking was observed within 2 years of the completion of the building, particularly in the foundation walls, slabs in the parking areas, and the main beams and columns on the ground floor. A partial cross section of the building is shown in Fig. 1 where extensive damage was observed.[1] Of particular interest were the foundation walls and the ground-floor beams. The foundation walls retained up to 5 m of backfill. Horizontal flexural cracks in these walls were observed in the zone of maximum moment and were 0.3 to 0.5 mm in width. The shear cracks in the beams were observed at several locations, and their width was as large as 0.8 mm. The source of these cracks was traced partially to excessive differential settlement of the foundation. A solution was thus required to improve the deformability of the structure in addition to its strength.

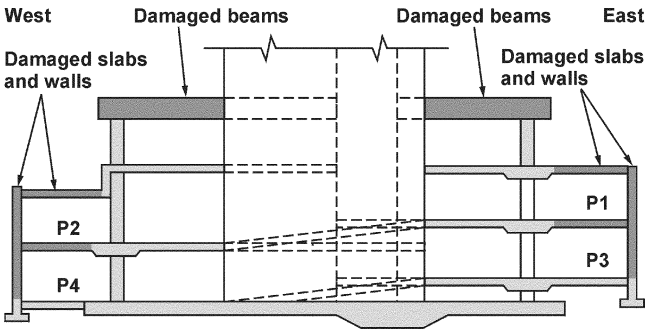

Fig. 1—Partial building cross section.

Numerous studies have been carried out in the last few years on the use of FRP in concrete structures,[2-7] particularly for the strengthening of individual members. Most of the specimens tested in various laboratories represented small-scale models of the prototypes. While in some cases the damaged specimens were repaired under load, most of the specimens were retrofitted with FRP while they carried no imposed loads. Other variations between the experimental investigations are the types of FRP materials used and their mechanical characteristics. The study reported herein used full-scale or near-full-scale models of walls and beams with the main objective of developing retrofitting techniques for damaged members using FRP. The effectiveness of the retrofitting with FRP was evaluated by comparing the performance of the repaired specimens with that of companion original specimens. Retrofitting was carried out while the specimens were under load and displayed the extent of damage similar to that observed in the field. Response of these specimens was also predicted using different analytical techniques. Based on the experimental and analytical work,

ACI Structural Journal, V. 99, No. 4, July-August 2002.
MS No. 01-289 received September 12, 2001, and reviewed under Institute publication policies. Pertinent discussion will be published in the May-June 2003 *ACI Structural Journal* if received by January 1, 2003.

Shamim A. Sheikh, *FACI, is a professor of civil engineering at the University of Toronto, Toronto, Ontario, Canada. He currently chairs Joint ACI-ASCE Committee 441, Reinforced Concrete Columns, and is a member of ACI Committee 374, Performance-Based Seismic Design of Concrete Buildings. In 1999, he received the ACI Structural Research Award for a paper on the design of ductile concrete columns. His research interests include earthquake resistance and seismic upgrade of concrete structures, confinement of concrete, use of fiber-reinforced polymer in concrete structures, and expansive cement and its applications.*

David DeRose *is involved in the new design and restoration of building enclosures at Halsall Associates Ltd. in Toronto. He received his MASc in civil engineering in 1997 from the University of Toronto. His research interests include retrofitting with fiber-reinforced polymers.*

ACI member **Jamil Mardukhi** *is a principal of NCK Engineering, Ltd., Toronto. His research interests include design and construction of special structures.*

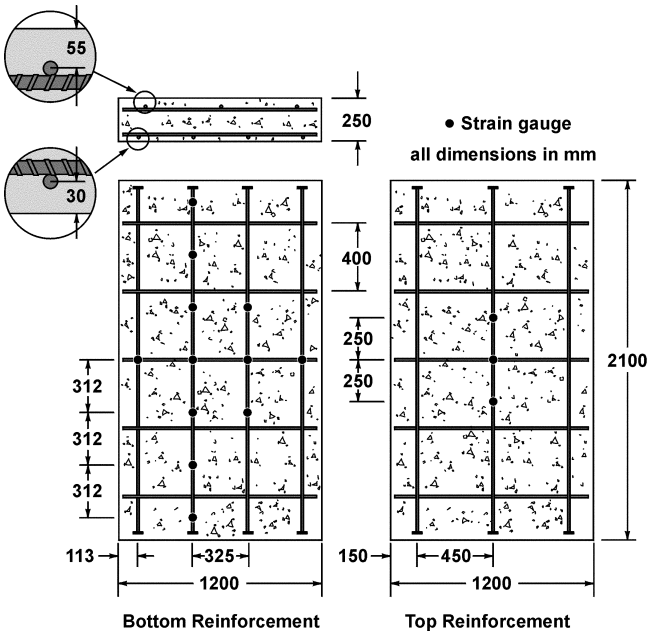

Fig. 2—Wall-slab specimen details.

retrofitting schemes were designed for various components of the building structure.

EXPERIMENTAL PROGRAM

Three wall-slab specimens and two beam specimens were constructed and tested. The three slab specimens were cast together and each beam was cast separately.

Wall-slab specimens

Each of the wall-slab specimens was 250 mm thick, 1200 mm wide, and 2.1 m long, representing a full-scale model of the foundation wall. Reinforcement in the direction of span consisted of four 10M (100 mm^2) bottom bars and three 10M top bars. Transverse reinforcement was provided by five 10M top-and-bottom bars. Small steel plates (40 x 25 mm) were welded to the ends of the longitudinal bars to ensure anchorage. All dimensions and reinforcement detailing are provided in Fig. 2. Each wall-slab specimen was instrumented with 15 electric strain gages on the longitudinal bars. The location of gages are also shown in Fig. 2. Due to rough timber formwork, the bottom surfaces of the specimens were uneven. Because two of the three specimens were to be repaired with FRP, it was decided to grind the bottom surfaces to yield a smooth, clean surface that would ensure a good bond between the concrete and the FRP.

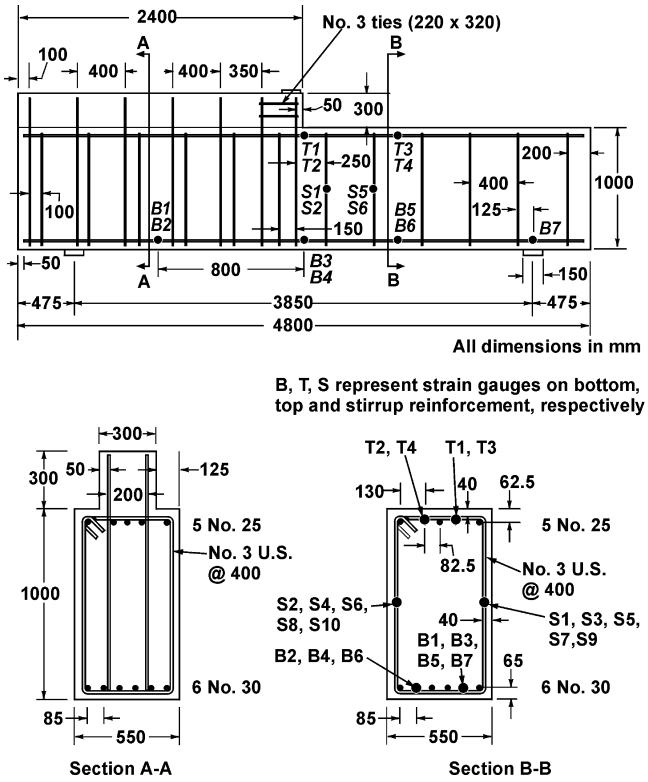

Fig. 3—Beam specimen details.

Beam specimens

Figure 3 shows the dimensions and reinforcement details of the beam specimens in which the test section was 1000 mm deep and 550 mm wide, a 5/6th-scale simulation of the beams in the building. The beam was scaled down slightly to accommodate construction in the laboratory. The beams in the building were framed into walls. This was simulated by building a haunched region and increasing the amount of reinforcement for that half of the beam. As a result, shear failure was expected in the shallower part of the beam (Section B-B in Fig. 3), similar to what has been observed in the field.

Each beam specimen contained 21 electric strain gages installed on the longitudinal and transverse steel. The locations of these gages are also shown in Fig. 3. The wooden framework was prepared to cast one specimen at a time. The casting was carried out in two steps. In the first step, the beam was cast without the haunch. Soon after casting, the specimen was covered with moist burlap and polyethylene sheeting for 3 days. At this point, the additional formwork was built to cast the haunched portion. The surface of the existing concrete at the cold joint was roughened before the new concrete was placed. Once again, the specimen was cured with wet burlap and polyethylene sheeting for 3 days after casting. Eight cylinders were also cast for each specimen to provide compressive strength data.

Concrete

Ready-mixed concrete with a specified compressive strength of 30 MPa and 20 mm maximum-size coarse aggregate was used. The strength of concrete in the wall-slab specimens varied between 48.4 and 53.9 MPa, while in the two beam specimens, the strength was 44.7 and 45.7 MPa.

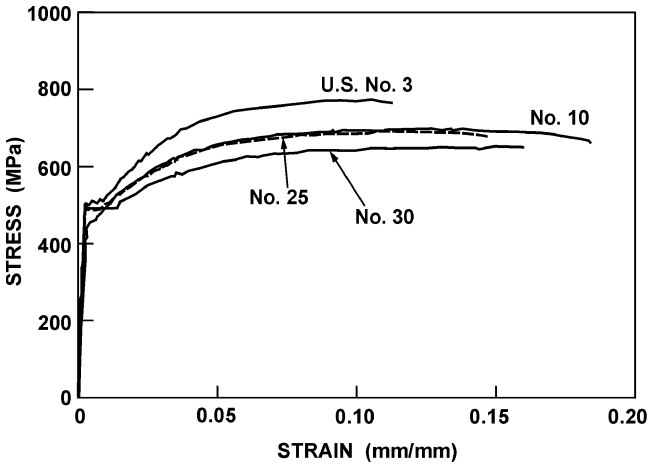

Fig. 4—Tensile stress-strain characteristics of steel.

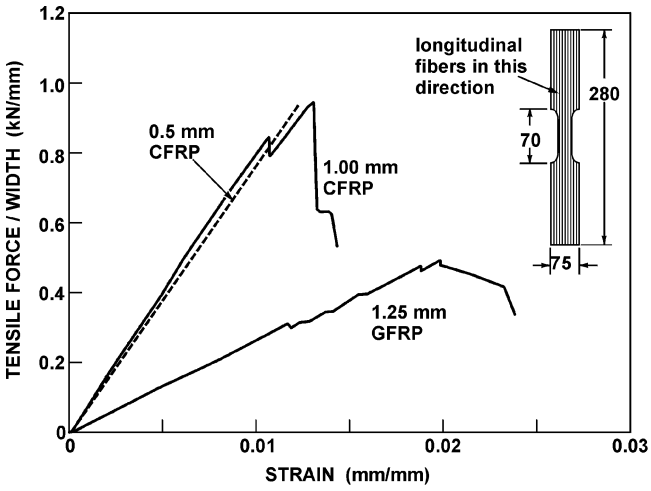

Fig. 5—Tensile load-strain behavior of FRP.

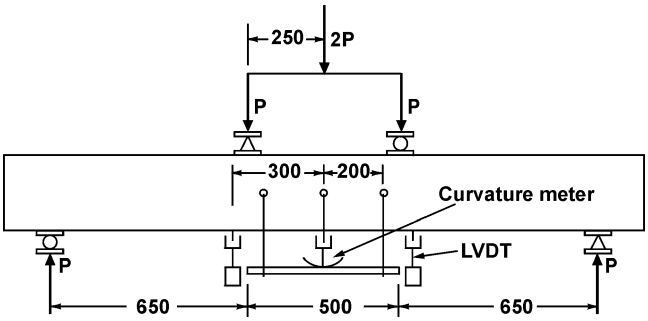

Fig. 6—Loading and support conditions for wall-slab specimens.

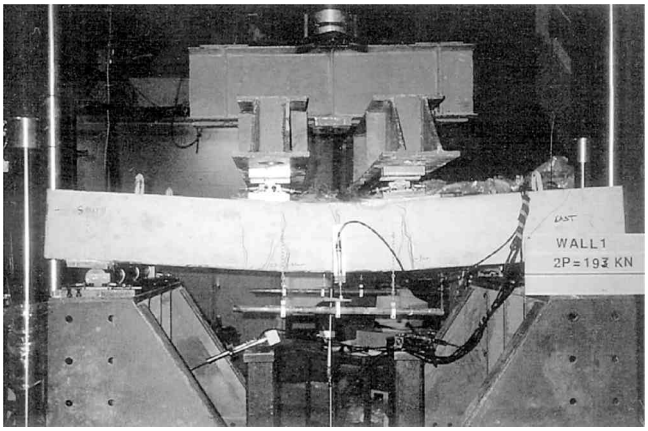

Fig. 7—Specimen Wall1 after failure.

Steel

Deformed bars were used in all the specimens. U.S. No. 3 (71 mm^2) bars were of Grade 60 steel, while Grade 400 steel was used for Canadian sizes 10M, 25M, and 30M (100, 500, and 700 mm^2). Figure 4 shows the stress-strain curves for the steel bars used in the test program. Each curve represents the average of a minimum of three tension tests.

Fiber-reinforced polymer

A commercially available FRP system was used for repairing the beam and wall-slab specimens. Two types of fabrics were used in this study. The glass fabric was nominally 1.25 mm thick, and the carbon fabric was designated as 1.0 mm thick. The test coupons for FRP were made from the fabric impregnated with epoxy and cured to harden. Two types of epoxies were used in the test; one of these was more viscous than the other. Each epoxy consisted of two components, A and B, that were mixed for 5 min. with a mixer at a speed of 400 to 600 rpm. Details of the test coupons and the load-strain curves for the two types of FRP are shown in Fig. 5. Each curve is an average of at least three tests. Because the thickness of the composite specimen depends on the amount of epoxy used, the tensile strength is represented in force per unit width instead of force per unit area, that is, stress.

TESTING

Wall-slab specimens

The three wall-slab specimens were tested under deformation control in a 2700 kN universal testing machine. Two line loads were applied to the specimens to produce flexural cracking similar to that observed in the field. The loading, support conditions, and the external instrumentation are shown in Fig. 6. Two curvature meters and three linear variable differential transducers (LVDTs) were used to obtain information about deformations during loading in addition to the strain gages installed on the steel cages. The cracks, as they developed under load, were also monitored in specimen Wall1 to determine the point at which the other two specimens (Wall2 and Wall3) would be repaired. Specimen Wall1 failed in flexure at a total load of 193 kN (Fig. 7).

Specimen Wall2 was to be rehabilitated with the carbon fabric. This specimen was initially loaded to 135 kN. The average strain at the center of the bottom flexural steel was 3.3×10^{-3} at this stage. Two flexural cracks had formed at this load. The crack width at various locations varied between 0.3 and 0.7 mm at the bottom of the slab with an average width of approximately 0.4 mm. These cracks were similar to those measured in the field. As a result, the displacement was maintained at the level while the repair was carried out by the supplier of the FRP composite material. All external instrumentation was removed to apply the fabric.

For the application of FRP to the underside of the slab, two types of epoxies were used as discussed previously. The more-viscous epoxy was applied directly to the concrete surface. This tacky coat of epoxy was essential to ensure that the fabric would adhere to the underside of the slab. The carbon fabric was saturated with the less-viscous (regular)

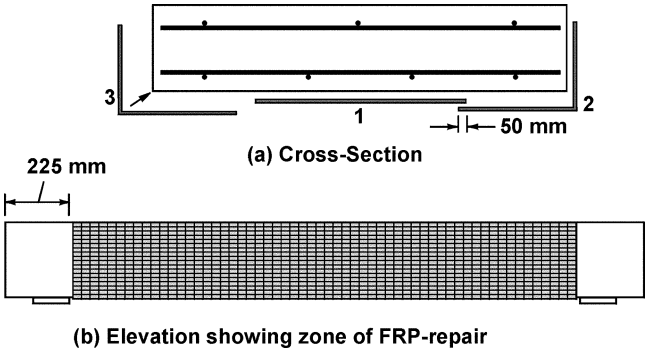

Fig. 8—Application of FRP on wall-slab specimens.

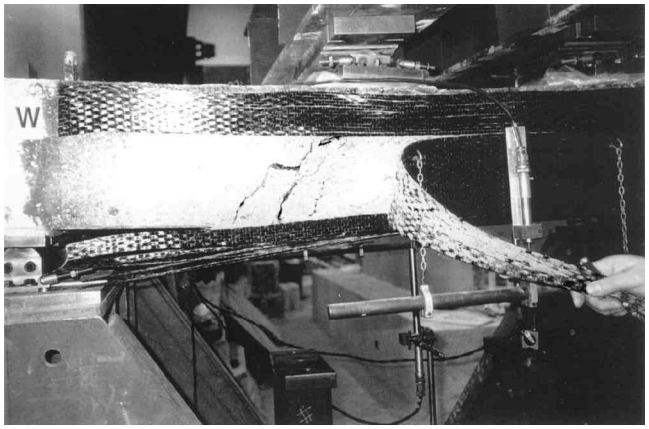

Fig. 9—Specimen Wall2 after failure.

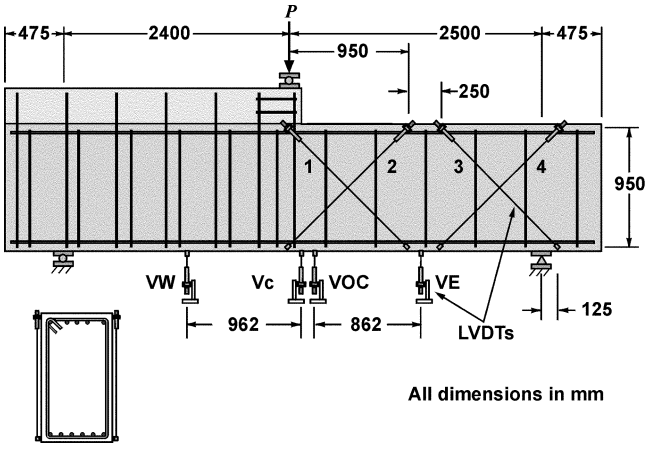

Fig. 10—Loading and support conditions for beam specimens.

epoxy prior to its application to the slab surface. Three strips of fabric, approximately 600 mm in width, were used as shown in Fig. 8. The outer strips of fabric were folded up and bonded to the sides of the specimen. Previous research[5] had shown that this provided an effective anchorage in beams to eliminate premature FRP separation from concrete. In the field, sufficient anchorage length was available to develop full strength of FRP. The epoxy was allowed to cure for 3 days before the repaired specimen was tested. During the time of repair and curing, the load fell to approximately 115 kN under constant displacement mode of the testing machine. At this time, the external instrumentation was reapplied, and the load was increased until the specimen was damaged

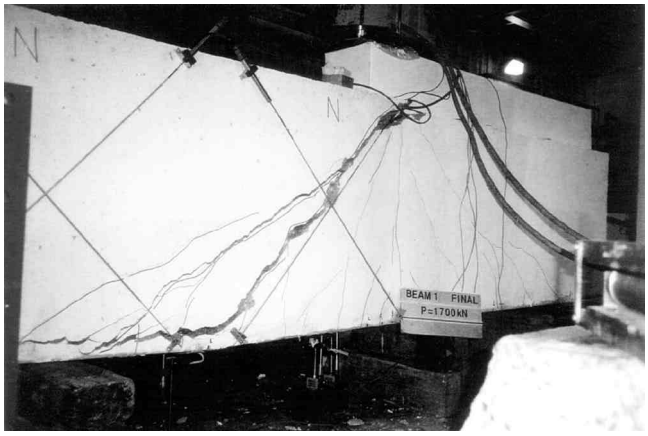

Fig. 11—Specimen Beam1 after failure.

extensively. The specimen failed in shear with large inclined cracks and delamination of CFRP (Fig. 9). The maximum load carried by the specimen was 478 kN.

The third specimen (Wall3) was tested the same way as Wall2, except that glass FRP (GFRP) was used for repair. The behavior of Wall3 was similar to that of Wall2, but the failure load was smaller. Shear failure occurred at the applied load of 422 kN.

Beam specimens

Both the beams were tested using a hydraulic jack connected to a rigid, 5400 kN testing machine frame. A load cell connected to the data acquisition system was used to measure the applied load. A single-point load was applied on the haunched portion (Fig. 10) to test the beam and produce cracking similar to that encountered in the field. External instrumentation, shown in Fig. 10, was used to obtain information about the shear strain and the deflection profile as the test progressed.

The first specimen, Beam1, was considered as a control specimen against which the performance of FRP-retrofitted beam was to be measured. Figure 11 shows the tested Beam1. As the load was increased, several shear cracks appeared that were monitored to determine the similarity of distress between the specimen and the beams in the building. At a load of approximately 1000 kN, extensive shear cracking was observed, with the maximum crack width equal to 0.75 mm. As the load increased to 1600 kN, the crack widths exceeded 2.0 mm, and the beam failed in a brittle manner at a load of 1700 kN. This mode of failure is typical of large beams that are shear-critical and contain very light shear reinforcement.

In addition to providing information about the safety of the beam in the field, the crack monitoring also helped identify the point at which the second beam specimen would be retrofitted with CFRP. The haunched region of the second beam was strengthened in shear by using a clamp consisting of steel beams and steel bars. This was done to ensure that this portion of the beam would not fail in shear after the repair of the test region had taken place.

Beam2 was loaded to 1180 kN when five diagonal cracks, ranging in width from 0.2 to 0.8 mm, were observed. The average strain at the center of the bottom flexural steel was approximately 1.5×10^{-3} at this stage. The crack pattern and the crack widths appeared similar to what was observed in the beams of the building. As a result, the displacement imposed

on the beam was maintained while the repair procedure was initiated by first removing all the external instrumentation.

The beams in the field were located such that, in the damaged zones, the FRP could be wrapped around the section. After mixing two parts of the epoxy as described previously, it was initially applied to the concrete surface with a roller. The carbon fabric was then saturated in the epoxy and wrapped around the beam section. Three strips of fabric, approximately 610 mm in width, were applied to the specimen as shown in Fig. 12. A fabric overlap of 200 mm was used at the top of the specimen. The specimen remained under load for 3 days for the duration of repair and curing of epoxy. The load during this time dropped from 1180 kN to approximately 1000 kN. After reinstalling the instrumentation at this time, the loading commenced.

At a load of 1911 kN, concrete in the haunched portion just below the load started to fail. This necessitated the unloading of the beam to repair the damaged area. The damaged concrete was removed. A steel enclosure was constructed and attached to specimen using threaded rods. The enclosure was filled with high-strength mortar and cured for 4 days. During reloading of the beam to 2470 kN, the beam behaved in an extremely ductile manner. The specimen was slightly unloaded a few times during this loading sequence as several LVDTs approached their limits and had to be reset to continue to capture the substantial deformations that were observed. The CFRP retrofitting was effective in enhancing the shear capacity of the beam and thus changed the brittle response to a very ductile one.

At a load of 2473 kN, the beam had deformed to such an extent that one of the support plates below the specimen was close to falling off its roller. The beam deflection at this point was approximately 110 mm. The specimen was unloaded again to readjust the plate. Testing soon resumed and the maximum load reached 2528 kN, corresponding to a deflection of 143 mm. Although all the strain gages had stopped working at this stage, there was enough evidence to state that the flexural steel was past strain hardening. In fact, the final failure would have been caused by the rupture of the bottom steel had it not been due to the rupture of the carbon fabric at a top edge close to the applied load, as shown in Fig. 13. Before the repair was carried out, the sharpness of the edges was somewhat reduced by slight grinding. A well-rounded edge perhaps would have eliminated this type of CFRP rupture.

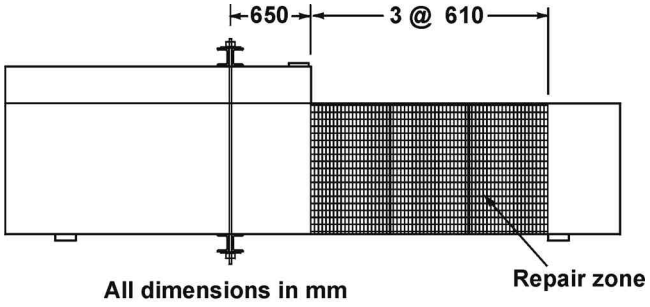

(a)

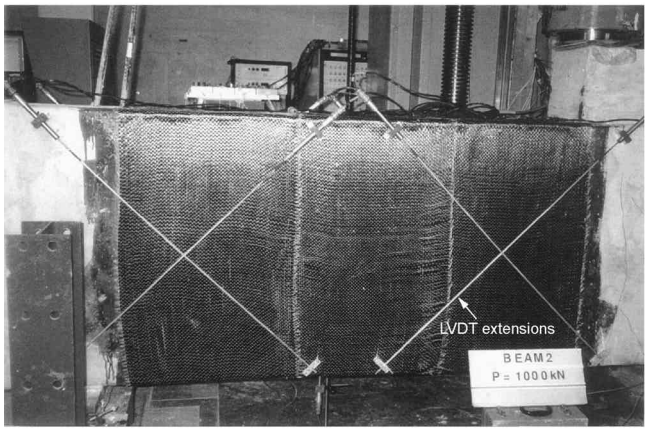

(b)

Fig. 12—Application of FRP on beam specimens.

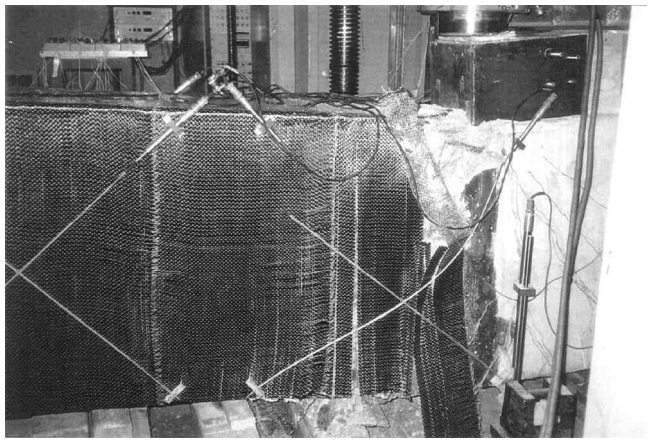

Fig. 13—Specimen Beam2 after failure.

RESULTS AND DISCUSSION

Wall-slab tests

The load-versus-maximum-deflection curves for the three specimens are presented in Fig. 14. Although the use of FRP resulted in a substantial increase (119% for GFRP and 148% for CFRP) in the ultimate capacity of the slabs, the full potential of FRP was not realized in either of the two repaired slabs. The external FRP reinforcement was specifically aimed at maximizing the enhancement in the flexural capacity of the slabs without causing premature bond failure of FRP or it to peel off from the concrete surface. The load corresponding to the shear capacity was much lower (50 to 68%) than that to the enhanced flexural capacity. The failure in both repaired slabs was, therefore, caused by shear. Table 1 shows the experimental and analytical failure loads and moment values. For Wall1, the analytical moment capacity was calculated by hand-calculation using the code provisions.[8-10] For the repaired specimens, Wall2 and Wall3, the analytical values were based on the shear capacity calculated according to the general method of the Canadian Code.[8]

In the CFRP-repaired specimen (Wall2), the load calculated based on the shear capacity was 484 kN, while the specimen failed at 478 kN. For the GFRP-repaired specimen (Wall3), the calculated and test failure loads were 430 and 422 kN, respectively. Close agreement between the test and theoretical values indicate that the FRP did not delaminate from the concrete until after the stress failure had taken place. The FRP wraps on the sides of the slabs were effective in eliminating premature FRP separation from the concrete. As indicated by a comparison of the analytical and experimental loads, presence of FRP on the sides of the slabs did not affect

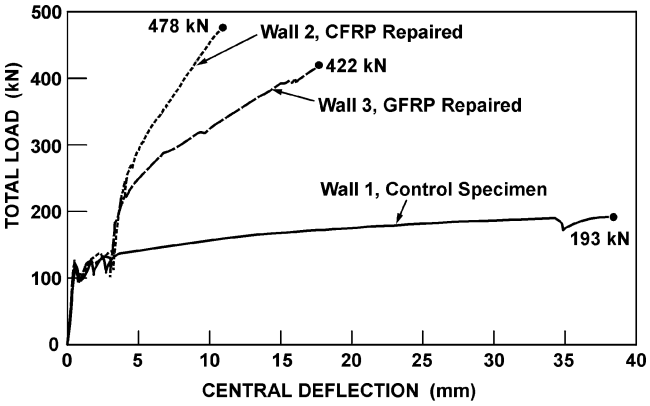

Fig. 14—Load-deflection behavior of wall-slab specimens.

Table 1—Load and moment values at failure in wall-slab specimens

Specimen	Experimental		Analytical		Failure mode
	Load, kN	Moment, kN-m	Load, kN	Moment, kN-m	
Wall1	193	62.7	182	59.1	Flexure
Wall2	478	155.4	484	157.3	Shear
Wall3	422	137.2	430	139.8	Shear

their mechanical behavior. The repair procedure restored the stiffness values of the slabs to that of the original, undamaged specimen (Fig. 14). The response of both the repaired specimens was reasonably ductile and resulted in a large energy dissipation, though not as ductile as the control specimen. The GFRP-repaired specimen showed higher ductility than the CFRP-repaired specimen. If higher ductility, rather than the strength, is desired, a lesser amount of FRP reinforcement than that used in the tests should be applied.

From the available analytical procedures based on strain compatibility, the moment-curvature responses of the three wall-slab specimens were developed. The Hognestad parabolic curve for the concrete stress-strain curve was used along with the steel and FRP properties shown in Fig. 4 and 5, respectively. In addition to hand-calculations, a computer program developed at the University of Toronto, RESPONSE,[9,11] was used to calculate the analytical response. For Wall1, hand-calculations were performed without tension-stiffening effects, with a tension-stiffening factor of 0.5. As shown in Fig. 15, the yield and the ultimate moment capacities are better predicted by ignoring the tension-stiffening factor. RESPONSE adjusts the effect of tension stiffening based on the information provided about the section. For the control specimen, the analytical responses match the experimental behavior very well.

In the repaired specimens, the initial curvature at the time of repair was considered in the analysis by allowing for the initial strains in the slab section. The strain in the bottom of the slab section thus became the locked-in strain difference between the concrete and FRP. Typical strain profiles encountered in the analysis have also been included in Fig. 15. RESPONSE allows the user to enter initial strains. As a result, two analyses were performed for each repaired specimen: the first up to the repair point; and the second after the repair, considering initial strain and addition of FRP. The analytical curves from RESPONSE shown in Fig. 15 are the curves obtained from merging the results from the two analyses. The initial

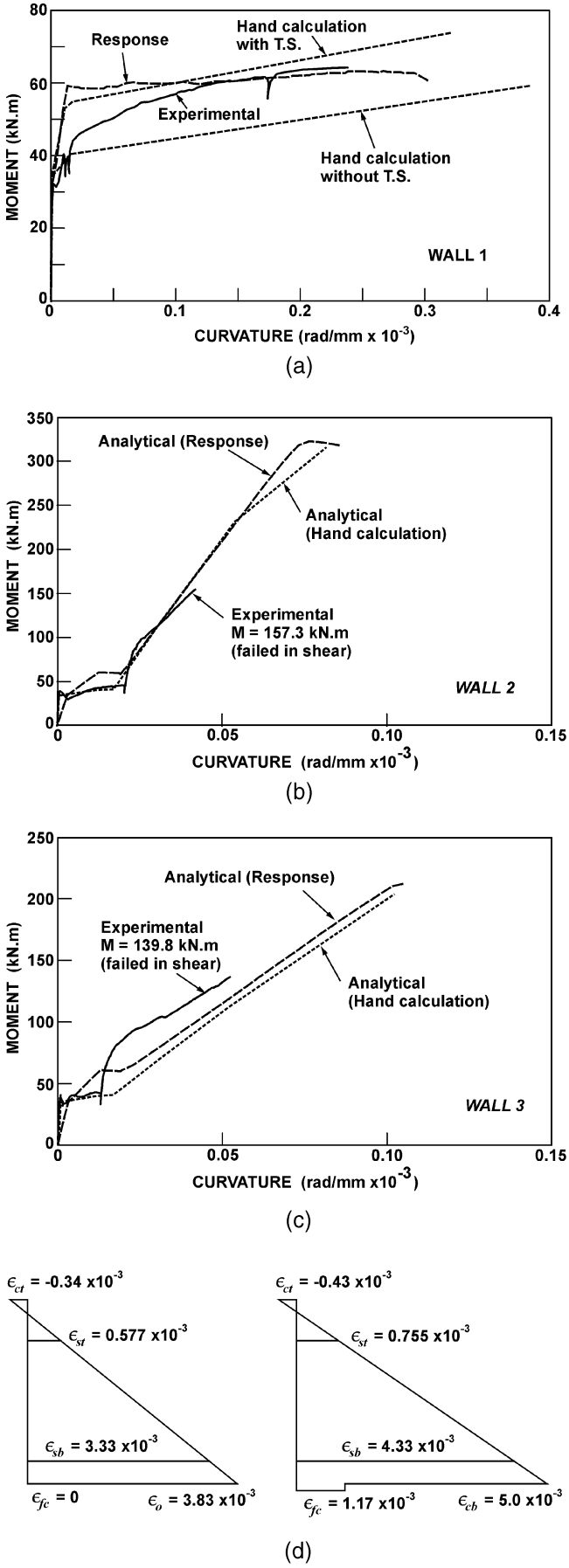

Fig. 15—Experimental and predicted responses of wall-slab specimens.

experimental behavior of the GFRP-retrofitted wall-slab specimen (Wall3) was somewhat stiffer than predicted, which may be the result of a lower-than-actual stiffness value used for GFRP in the analysis. Overall analytical curves, however, predict the behavior reasonably well up to the failure of the specimen when both the specimens failed in shear. The analytical curves are shown to a point where a quick drop in load was observed. The moment values corresponding to the shear capacity, predicted by the general method of the Canadian Code,[8] are given in Table 1. It can be concluded that the available techniques with appropriate material properties can be used to evaluate the performance of slabs repaired in flexure with FRP.

Beam tests

The load-deflection curves for the two beams are shown in Fig. 16. While Beam1 failed in shear at a load of 1700 kN, Beam2, retrofitted with CFRP, had an ultimate capacity of 2528 kN and failed in flexure. The maximum deflection at failure in the original beam was 14 mm under the load point, which increased to 143 mm in the repaired beam. The repaired beam was retrofitted with CFRP for shear resistance under a load of 1180 kN when the maximum beam deflection was less than 8 mm. The energy dissipation capacity, or the toughness, of the repaired beam was more than 2600% of that of the original beam.

The failure load for the control beam, based on the shear capacity calculated from the Canadian Code,[8] was between 1095 kN (simplified method) and 1167 kN (general method). The beam capacity calculated from the ACI code[10] equations is 1561 kN. Load estimates from both the codes were conservative, as the shear failure of the beam occurred at a load of 1700 kN.

The shear span-depth ratio of the beam was approximately equal to 2.0, which may have contributed to the development of compression struts after significant cracking had occurred.[9] This may have contributed to the larger shear capacity observed in the test. The capacity based on the modified compression field theory was calculated to be 1710 kN,[12] which is reasonably close to the test value.

For the application of code equations to predict the shear capacity of the repaired beam, the carbon fabric was considered as a series of equivalent stirrups. The total failure load, based on the general method of the Canadian Code,[8] was 5245 kN. The predicted failure load, based on shear capacity according to the simplified method of the Canadian Code and the ACI Code,[10] was 4985 kN. The beam, however, failed in flexure at a load of 2528 kN. The moment-curvature response of the beam section subjected to the maximum moment is shown in Fig. 17 along with the behavior obtained from the test. The two curves agree quite well. It should be noted that the analytical moment-curvature response, shown in Fig. 17, is for a steel-reinforced section and is unaffected by the presence of FRP. As mentioned previously, retrofitting was required to enhance strength as well as deformability of the structure. The FRP wraps that were wrapped around the section not only increased the shear capacity of the beam, but also enhanced the deformation capacity of the concrete in compression, resulting in large flexural ductility. In situations where complete wrapping of a section is not possible, the bonding between concrete and FRP must be ensured to obtain strength enhancement.

Figure 18 shows the shear force-shear strain response of a section approximately 475 mm from the load application

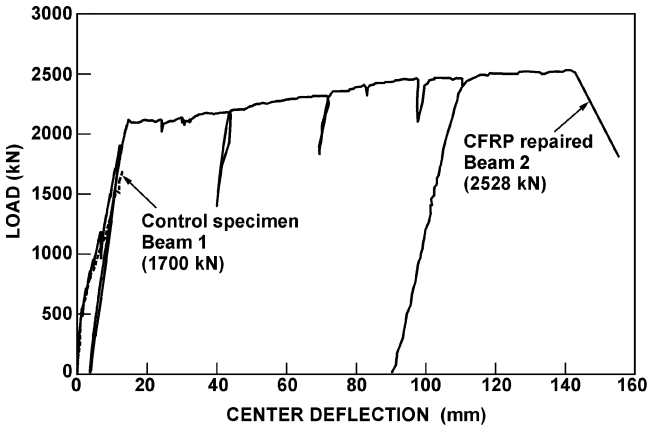

Fig. 16—Load-deflection behavior of beam specimens.

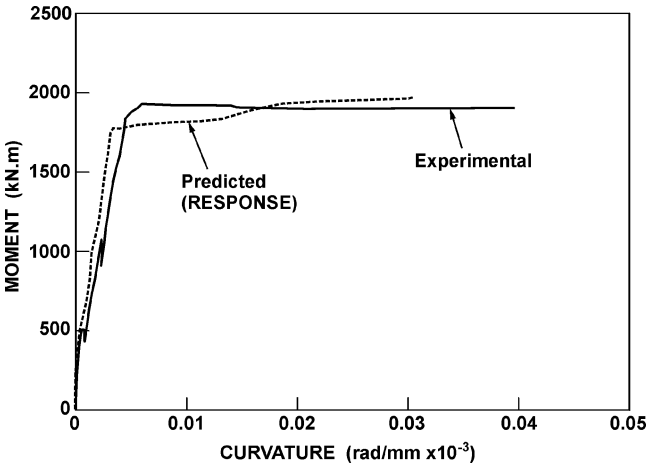

Fig. 17—Experimental and predicted responses of specimen Beam2.

point in Beam1, as obtained from the test. A similar behavior was also measured for a section 1675 mm from the load point in the test region of the beam. This section was at the intersection of one set of the diagonal LVDTs used to calculate the shear strain. Analytical behavior curve using RESPONSE for this section is also shown in Fig. 18. The initial portion of the measured and predicted curves match quite well. The predicted shear capacity of less than 600 kN, however, is considerably lower than the measured capacity of 805 kN. A compressive strut may have formed that influenced the behavior after substantial cracking had occurred. Predicted and measured shear capacities were similar at a section 1675 mm away from the load.

Measured and predicted shear plots for the repaired specimens are shown in Fig. 19 for a section approximately 475 mm from the load point. An analytical curve obtained from RESPONSE provided a reasonably accurate simulation of the section's behavior. The carbon wrap prevented the widening of shear cracks, which allowed the concrete contribution to shear resistance to be maintained. With additional shear capacity from CFRP, the beam was able to develop full flexural capacity and large deformation before failure. Although the fabric ruptured at a corner initiating the final failure of the beam, it can be argued that this may have been triggered by very large flexural deformations.

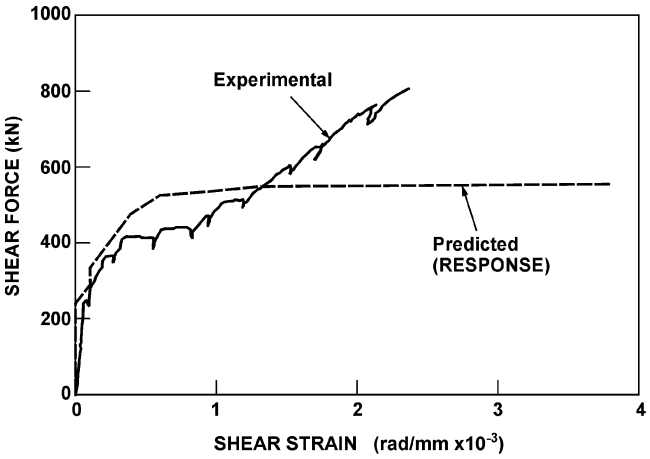

Fig. 18—Predicted and measured shear response of Beam1.

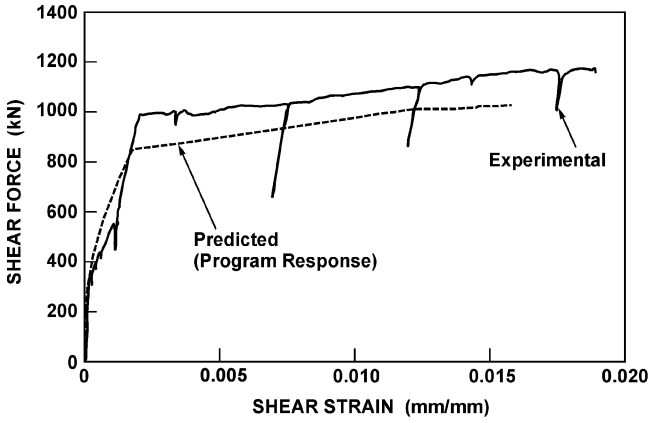

Fig. 19—Predicted and measured shear responses of Beam2.

SUMMARY AND CONCLUSIONS

The structural distress encountered at various locations in a multistory building was simulated in near full-scale specimens in the laboratory. Specimens were damaged to the same degree as the prototype structural members in the field, and the repair was carried out under load using CFRPs and GFRPs. The repaired specimens were tested to failure. Companion control specimens were also tested to failure without rehabilitation to provide a basis for comparison and evaluate the effectiveness of the repair techniques. Because the damage to the building was partly caused by excessive differential foundation settlement, enhancement in ductility was one of the main focuses in designing the retrofitting schemes, particularly in the case of beams showing signs of failure in shear. Another factor in the selection of the repair technique was the continued use of the structure for normal activities.

The experimental program included testing of three wall-slab specimens and two beams. The wall-slab specimens were 250 mm thick, 1200 mm wide, and 1.2 m long, and the beams were 550 mm wide, 1000 mm deep, and 4.8 m long. Various analytical techniques were used to simulate experimental behavior of the specimens. The following conclusions can be drawn from the study.

Retrofitting with FRPs provides a feasible rehabilitation techniques for wall-slabs and beams. FRPs were effective in enhancing strength in both flexure and shear. No premature delamination of FRP was observed in the test specimens. Both carbon and glass composites provided significant enhancement (more than 148%) in flexural strength to the extent that the failure of the wall-slab specimens shifted to shear mode which, in some cases, may not be acceptable. If needed, the shear failure can be avoided by limiting the flexural strength enhancement—achieved by limiting the amount of FRP used. This will allow a more-efficient use of FRP and result in a more-ductile behavior.

The wrapping of the beam of section size 550 x 1000 mm with one layer of CFRP resulted in changing the brittle mode of shear failure at 1700 kN to a very ductile flexure failure at 2528 kN. The deflection at failure increased from 14 mm in the control specimen, to 143 mm in the retrofitted specimen. The theoretical failure load for the retrofitted beam based on its shear capacity was approximately 5000 kN.

The available analytical techniques provided reasonable simulations of the behavior of the specimens retrofitted with CFRP and GFRP. Provisions of the Canadian and ACI building codes[8,10] were found to provide reasonable estimates of the capacities for the retrofitted specimens.

ACKNOWLEDGMENTS

The experimental work reported herein was conducted with the financial assistance from the Natural Sciences and Engineering Research Council under Grant No. STR 195771. The tests were conducted in the Structures Laboratories at the University of Toronto. Technical and financial assistance from R. J. Watson, Inc., of East Amherst, N.Y., Fyfe Co. of San Diego, Calif., and RoadSavers Central Ltd. of Toronto, is gratefully acknowledged.

REFERENCES

1. DeRose, D., and Sheikh, S.A., "Rehabilitation of a Concrete Structure using Fibre-Reinforced Plastics," *Research Report*, Department of Civil Engineering, University of Toronto, Toronto, Ontario, Canada, 1997, 170 pp.

2. Mufti, A. A.; Erki, M.; and Jaeger, L. G., *Advanced Composite Materials with Applications to Bridges*, Canadian Society of Civil Engineering, 1991, 297 pp.

3. Meier, U., and Kaiser, H., "Strengthening of Structures with CFRP Laminates," *Advanced Composite Materials in Civil Engineering Structures*, Proceedings of the Speciality Conference, Las Vegas, Nev., ASCE, Jan. 31-Feb. 1, 1991, pp. 288-301.

4. Saadatmanesh, H., and Ehsani, M., "RC Beams Strengthened with GFRP Plates: Part I and Part II," *Journal of Structural Engineering,* ASCE, V. 117, No. 11, 1991, pp. 3417-3455.

5. Sharif, A.; Al-Sulaimani, G. J.; Basunbul, I. A.; Baluch, M. H.; and Bhaleb, B.N., "Strengthening of Initially Loaded Reinforced Concrete Beams using FRP Plates, *ACI Structural Journal*, V. 91, No. 2, Mar.-Apr. 1994, pp. 160-168.

6. Fam, A. Z., and Rizkalla, S. H., "Behavior of Axially Loaded Concrete-Filled Circular Fiber-Reinforced Polymer Tubes," *ACI Structural Journal*, V. 98, No. 3, May-June 2001, pp. 280-289.

7. Shahawy, M.; Chaallal, O.; Beitelman, T. E.; and El-Saad, A., "Flexural Strengthening with Carbon Fiber-Reinforced Polymer Composites of Preloaded Full-Scale Girders," *ACI Structural Journal*, V. 98, No. 5, Sept.-Oct. 2001, pp. 735-743.

8. "Code for the Design of Concrete Structures for Building (CAN3-A23.3 M94)," Canadian Standards Association, Rexdale, Ontario, Canada, 1994, 199 pp.

9. Collins, M. P., and Mitchell, D., *Prestressed Concrete Basics*, Canadian Prestressed Concrete Institute, 161 pp.

10. ACI Committee 318, "Building Code Requirements for Structural Concrete (ACI 318-99) and Commentary (318R-99)," American Concrete Institute, Farmington Hills, Mich., 1999, 391 pp.

11. Bentz, E., "Sectional Analysis of Reinforced Concrete Members," PhD thesis, Department of Civil Engineering, University of Toronto, Toronto, Ontario, Canada, Jan. 2000, 310 pp.

12. Sheikh, S. A.; Vecchio, F. J.; DeRose, D.; and Bucci, F., "Behavior and Analysis of FRP-Repaired Elements," *Proceedings of the International Conference on High Performance High Strength Concrete*, Perth, Australia, Aug. 10-12, 1998, pp. 669-684.

APPENDIX I—EXAMPLE

A beam 12 x 24 in. (305 x 610 mm) in section shown in Fig. 20(a) is to be retrofitted with CFRP to enhance its flexural and shear capacity by 40%. At the time of retrofitting, the applied moment at the section was 1230 k-in. (139 kN-m). Concrete compressive strength is 4000 psi (27.6 MPa), steel yield strength is 60,000 psi (414 MPa), and FRP ruptures at 5000 lb/in. (875 N/mm) width at a strain of 0.015.

Solution

Retrofitting for flexure—Based on simple hand-calculations, it can be shown that the cracking, yielding of tension steel, and the ultimate conditions occur at the following moment and curvature values.

	Moment k-in (kN-m)	Curvature $\times 10^{-6}$/in (10^{-6}/mm)
cracking	546 (61.7)	10.8 (0.43)
yielding	1955 (220.9)	140.0 (5.51)
ultimate	2088 (235.9)	1023.0 (40.28)

Corresponding to the applied moment of 1230 k-in. (139 kN-m), the strain profile at the section is as shown in Fig. 20(b). The curvature value at this stage is 84.4×10^{-6}/in. (3.32×10^{-6}/mm). The beam section has cracked but the tension steel has not yielded.

At this stage, the installation of CFRP at the bottom of the beam would mean that the tensile strain in concrete at the bottom would be larger than the strain in CFRP by 1.53 millistrain. Any additional moment in the beam would now be resisted by additional compression in concrete, and additional tension in steel until it reaches yield and tension in CFRP. The strain profile at ultimate condition of the beam retrofitted with a 10 in. (254 mm) wide CFRP sheet is shown in Fig. 20(c). It should be noted that the strain in CFRP is 0.01247 (0.014 – 0.00153). The tension steel has yielded and the concrete has failed in compression. The ultimate moment capacity is 2943 k-in. (332.6 kN-m) and the corresponding curvature is 708×10^{-6}/in. (27.87×10^{-6} mm).

Figure 20(d) shows the moment-curvature responses of the original and retrofitted reactions. The moment capacity has increased by approximately 41% as a result of retrofitting, but the ultimate curvature has reduced by approximately 31%.

Retrofitting for shear—Original beam

$$Vs = 2\sqrt{f_c'}\,bd = 31{,}876 \text{ lb } (141.8 \text{ kN})$$

$$V_s = A_v f_y \frac{d}{s} = \frac{0.22(60{,}000)(21)}{10.5} = 26{,}400 \text{ lb } (117.4 \text{ kN})$$

$$Vu = Vc + Vs = 58.3 \text{ kips } (259.2 \text{ kN})$$

To increase shear capacity of the beam by 41% (same enhancement as in flexure), the FRP reinforcement will be required to provide 23.9 kips (106.3 kN) of shear resistance.

$$V_{FRP} = A_f f_f \frac{d}{s}$$

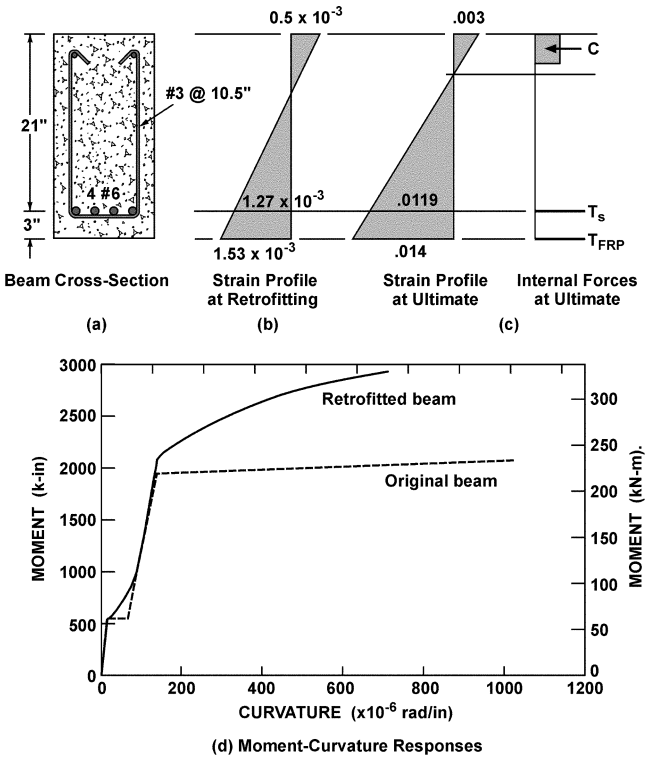

Fig. 20—Example.

$A_f = 2tw$, where t is the thickness of FRP fabric, and w is the width of FRP stirrup

$$V_{FRP} = 2tw\frac{5000}{t} \times \frac{21}{s}$$

$$= 210{,}000\,\frac{w}{s} \text{ lbs}$$

$$V_{FRP} = 210 \text{ kips}$$

$$23.9 = 21.0\frac{w}{s}$$

$$\frac{w}{s} = 0.114$$

where

s = 10 in.; and

w = 1.14 in.

For a larger factor of safety against shear compared to flexure, external FRP stirrups of 1.5 in. (38 mm) width can be used at 10 in. (254 mm) spacing.

Appropriate anchorage will be required for FRP sheets in both flexure and shear applications.